CENTRE FOR **STOCHASTIC GEOMETRY**
AND ADVANCED **BIOIMAGING**

Astrid Kousholt, Johanna F. Ziegel, Markus Kiderlen and Eva B. Vedel Jensen

Stereological estimation of mean particle volume tensors in $\mathbb{R}^3$ from vertical sections

No. 09, July 2016

Stereological estimation of mean particle volume tensors in $\mathbb{R}^3$ from vertical sections

Astrid Kousholt[1], Johanna F. Ziegel[2], Markus Kiderlen[1] and Eva B. Vedel Jensen[1]

[1]Department of Mathematics, Aarhus University, {kousholt,kiderlen,eva}@math.au.dk
[2]Department of Mathematics and Statistics, Institute of Mathematical Statistics and Actuarial Science, University of Bern, johanna.ziegel@stat.unibe.ch

Abstract

In this paper, we discuss stereological estimation of mean particle volume tensors in $\mathbb{R}^3$ from vertical sections. We consider a particle process of compact particles that can be represented as a stationary marked point process. Under the assumption that the particle distribution is invariant under rotations around a fixed axis, called the vertical axis, we show how the mean particle volume tensors can be estimated consistently (in a probabilistic sense) from observations in vertical sections through a sample of particles. In a simulation study, the new estimator has a superior behaviour compared to an earlier estimator based on observations in several optical planes.

1 Introduction

Volume tensors, or more generally Minkowski tensors, have been used with success for shape and orientation description of spatial structures in material science, see [3], [5], [11], [12]. An early example from the biosciences is given in [2].

Information about shape and orientation from tensors can fairly easily be determined if a 3D voxel image of the spatial structure under study is available. However, for biostructures like cells it is even in conventional microscopy difficult to construct such voxel images. For such cases, local stereological methods of estimating volume tensors from observations in planar sections have been developed in [9] and [13]. A particular focus has been on methods of obtaining information on shape and orientation for particle populations.

In this paper, we give an introduction to these methods and also present a new estimator that has great potential use in optical microscopy.

2 The particle model

Let X be a particle process of compact particles in $\mathbb{R}^3$. We assume that the process can be represented as a stationary marked point process

$$\{[x(K); K - x(K)] : K \in X\}.$$

Here, $x(K) \in K$ is a reference point associated to the particle $K \in X$ and the mark $K - x(K)$ is the particle translated such that its reference point is at the origin o. We let $\mathbf{K}_0$ be a random compact set with distribution equal to the particle mark distribution $\mathbb{Q}$, say. The random set $\mathbf{K}_0$ may be regarded as a randomly chosen particle or a typical particle with o as its reference point. The intensity of the marked point process, that is the mean number of reference points per unit volume, is denoted by λ. For a detailed description of stationary particle processes and the definition of the mark distribution, see [10, Chapter 3].

Our aim is to estimate the mean particle volume tensors $\mathbb{E}\Phi_3^{r,0}(\mathbf{K}_0)$ where the volume tensor of rank $r \in \mathbb{N}_0$ of a compact set K is given by

$$\Phi_3^{r,0}(K) = \frac{1}{r!} \int_K x^r \, \mathrm{d}x. \tag{2.1}$$

Here, for $x = (x_1, x_2, x_3) \in \mathbb{R}^3$, x^r is the rank r tensor that can be identified with an array of elements of the form

$$(x^r)_{i_1 i_2 i_3} = x_1^{i_1} x_2^{i_2} x_3^{i_3} \qquad \text{for } i_1, i_2, i_3 \in \{0, \ldots, r\} \text{ with } i_1 + i_2 + i_3 = r.$$

We thus identify the r-tensor $\Phi_3^{r,0}$ with its coefficients with respect to a suitably chosen basis. The integration in (2.1) is to be understood elementwise.

The estimation will be based on a sample of particles, collected as those particles with reference point in a full-dimensional compact sampling window W,

$$\{K \in X : x(K) \in W\}. \tag{2.2}$$

For an illustration of the sampling procedure, see Figure 1.

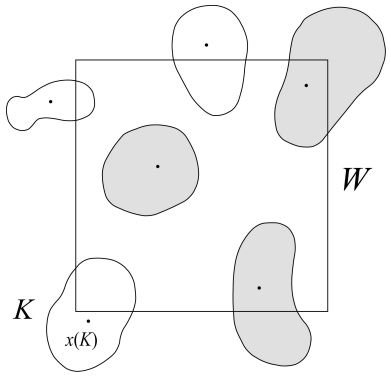

Figure 1: A particle K is sampled if its reference point $x(K)$ belongs to W. Sampled particles are shown hatched.

Due to the stationarity of the particle process X, we have for any integrable function f on compact subsets of $\mathbb{R}^3$

$$\mathbb{E} \sum_{K \in X,\, x(K) \in W} f(K - x(K)) = \lambda V_3(W) \mathbb{E}\, f(\mathbf{K}_0),$$

where V_3 denotes volume. If we let $N(W)$ be the number of sampled particles, it follows that

$$\frac{\mathbb{E} \sum_{K \in X,\, x(K) \in W} f(K - x(K))}{\mathbb{E} N(W)} = \mathbb{E}\, f(\mathbf{K}_0). \tag{2.3}$$

In particular if f in (2.3) equals the elements of $\Phi_3^{r,0}$, we find that

$$\frac{\sum_{K \in X,\, x(K) \in W} \Phi_3^{r,0}(K - x(K))}{N(W)} \tag{2.4}$$

is a ratio-unbiased estimator of $\mathbb{E}\Phi_3^{r,0}(\mathbf{K}_0)$. The estimator (2.4) is consistent (in a probabilistic sense) under weak assumptions on the particle process, see [4, Corollary 12.2.V] for the case of an ergodic process in an expanding window regime.

The estimator (2.4) requires that the volume tensor $\Phi_3^{r,0}$ can be determined on the sampled particles. If we do not have direct access to the particles in 3D, we need to develop stereological methods of estimating the volume tensors of the sampled particles from planar sections.

Stereological estimators of volume tensors based on observations in vertical slices have been derived in [9] and [13]. In a model-based setting, these estimators are valid under the *restricted isotropy assumption* where the distribution of the typical particle $\mathbf{K}_0$ is invariant under rotations around a line M in the Grassmannian $G(3,1)$ of one-dimensional linear subspaces in $\mathbb{R}^3$. The line M is called the vertical axis.

To be more specific, let $T = L + tB^3$ be a vertical slice. Here, L is a plane through the origin, containing M, and tB^3 is a ball centred at o and with radius t, see Figure 2. Let

$$\widehat{\Phi}_3^{r,0}(K) = \frac{1}{r!} \int_{K \cap T} x^r G(t^2 / |p_{M^\perp}(x)|^2)^{-1}\, \mathrm{d}x, \tag{2.5}$$

where G is the cumulative distribution function of the Beta distribution with parameters $(1/2, 1/2)$ and $p_{M^\perp}$ is the orthogonal projection on $M^\perp$. Then, cf. [13, Section 3 and Appendix A (online supporting information)],

$$\mathbb{E}\widehat{\Phi}_3^{r,0}(\mathbf{K}_0) = \mathbb{E}\Phi_3^{r,0}(\mathbf{K}_0),$$

and, combining this identity with (2.3),

$$\frac{\sum_{K \in X,\, x(K) \in W} \widehat{\Phi}_3^{r,0}(K - x(K))}{N(W)} \tag{2.6}$$

is a ratio-unbiased (and consistent) estimator of $\mathbb{E}\Phi_3^{r,0}(\mathbf{K}_0)$. This estimator will be called *the slice estimator* in the following.

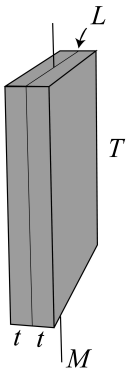

Figure 2: A vertical slice T of thickness $2t$. The central plane L contains the vertical axis M.

Note that under a restricted isotropy assumption, the mean particle volume tensors $\mathbb{E}\Phi_3^{r,0}(\mathbf{K}_0)$ do not vary freely. For $\mathbb{E}\Phi_3^{1,0}(\mathbf{K}_0)$ and $\mathbb{E}\Phi_3^{2,0}(\mathbf{K}_0)$, we have

$$\mathbb{E}\Phi_3^{1,0}(\mathbf{K}_0) \in M, \tag{2.7}$$

and

$$\mathbb{E}\Phi_3^{2,0}(\mathbf{K}_0) - \frac{(\mathbb{E}\Phi_3^{1,0}(\mathbf{K}_0))^2}{2\mathbb{E}\Phi_3^{0,0}(\mathbf{K}_0)} = B \begin{pmatrix} \eta & 0 & 0 \\ 0 & \mu & 0 \\ 0 & 0 & \mu \end{pmatrix} B^T, \tag{2.8}$$

where the first column of the orthogonal matrix B is a unit vector, spanning M ([13, p. 819]). The slice estimator may be adjusted such that constraints of this type are fulfilled ([13, p. 821–822]).

3 Stereological estimation from vertical sections

In this section, we will show that, under the restricted isotropy assumption, $\mathbb{E}\Phi_3^{r,0}(\mathbf{K}_0)$ can be estimated from observations only in the central plane L of the slice T. To the best of our knowledge, this estimator has not been described before.

To show this claim, we assume for simplicity that the vertical axis M is the z-axis and use cylindrical coordinates to obtain

$$\begin{aligned} \mathbb{E}\Phi_3^{r,0}(\mathbf{K}_0) &= \frac{1}{r!}\mathbb{E}\int_{\mathbf{K}_0} x^r \,\mathrm{d}x \\ &= \frac{1}{r!}\int_{z=-\infty}^{\infty}\int_{u=0}^{\infty}\int_{\theta=0}^{2\pi} P\big((u\cos\theta, u\sin\theta, z) \in \mathbf{K}_0\big) \\ &\qquad \cdot (u\cos\theta, u\sin\theta, z)^r u \,\mathrm{d}\theta \,\mathrm{d}u \,\mathrm{d}z. \end{aligned}$$

Using restricted isotropy, we get

$$\mathbb{E}\Phi_3^{r,0}(\mathbf{K}_0) = \frac{1}{r!}\int_{z=-\infty}^{\infty}\int_{u=0}^{\infty} P((u,0,z) \in \mathbf{K}_0) f_r(u,z) \,\mathrm{d}u \,\mathrm{d}z, \tag{3.1}$$

where $f_r(u,z)$ is the rank r tensor

$$f_r(u,z) = \int_{\theta=0}^{2\pi} (u\cos\theta, u\sin\theta, z)^r u \,\mathrm{d}\theta$$

for $u > 0$ and $z \in \mathbb{R}$. The elements of the tensor $f_r(u,z)$, $u > 0$, $z \in \mathbb{R}$, are given by

$$\begin{aligned} f_r(u,z)_{i_1i_2i_3} &= \int_0^{2\pi} u(u\cos\theta)^{i_1}(u\sin\theta)^{i_2} z^{i_3} \,\mathrm{d}\theta \\ &= u^{i_1+i_2+1} z^{i_3} \int_0^{2\pi} (\cos\theta)^{i_1}(\sin\theta)^{i_2} \,\mathrm{d}\theta \\ &= c_{i_1i_2} u^{i_1+i_2+1} z^{i_3}, \end{aligned}$$

say, for $i_1, i_2, i_3 \in \{0, \ldots, r\}$ with $\sum_{j=1}^3 i_j = r$, where

$$c_{i_1i_2} = \begin{cases} 2\dfrac{\omega_{i_1+i_2+2}}{\omega_{i_1+i_2+1}} \dfrac{\binom{(i_1+i_2)/2}{i_1/2}}{\binom{i_1+i_2}{i_1}}, & \text{for } i_1, i_2 \text{ even}, \\ 0, & \text{otherwise.} \end{cases}$$

Here, ω_i is the surface area of the unit sphere in $\mathbb{R}^i$. It follows that

$$\mathbb{E}\Phi_3^{r,0}(\mathbf{K}_0)_{i_1i_2i_3} = (r+1)c_{i_1i_2}\mathbb{E}\big[\Phi_{2,L}^{r+1,0}(\mathbf{K}_0 \cap L_+)_{i_1+i_2+1,i_3}\big], \tag{3.2}$$

where

$$\begin{aligned} L &= \{(u,0,z) : u, z \in \mathbb{R}\}, \\ L_+ &= \{(u,0,z) : u > 0, z \in \mathbb{R}\}, \end{aligned}$$

and $\Phi_{2,L}^{r+1,0}(\mathbf{K}_0 \cap L_+)$ is the rank $r+1$ volume tensor of $\mathbf{K}_0 \cap L_+$, considered as subset of L. Alternatively, one can use the larger set $\mathbf{K}_0 \cap L$ and obtain

$$\mathbb{E}\Phi_3^{r,0}(\mathbf{K}_0)_{i_1i_2i_3} = (r+1)\frac{c_{i_1i_2}}{2}\mathbb{E}\big[\Phi_{2,L}^{r+1,0}(\mathbf{K}_0 \cap L)_{i_1+i_2+1,i_3}\big].$$

If, for a compact set K, we let $\widetilde{\Phi}_3^{r,0}(K)$ be the rank r tensor with

$$\widetilde{\Phi}_3^{r,0}(K)_{i_1i_2i_3} = (r+1)\frac{c_{i_1i_2}}{2}\Phi_{2,L}^{r+1,0}(K \cap L)_{i_1+i_2+1,i_3},$$

we find

$$\mathbb{E}\widetilde{\Phi}_3^{r,0}(\mathbf{K}_0) = \mathbb{E}\Phi_3^{r,0}(\mathbf{K}_0)$$

and

$$\frac{\sum_{K\in X,\, x(K)\in W} \widetilde{\Phi}_3^{r,0}(K - x(K))}{N(W)} \tag{3.3}$$

is a ratio-unbiased (consistent) estimator of $\mathbb{E}\Phi_3^{r,0}(\mathbf{K}_0)$. This estimator will be called *the section estimator*.

The section estimator is much simpler to implement in microscopy than the slice estimator and, furthermore, it has technical advantages. For instance, the estimator is not sensitive to shrinkage in the direction perpendicular to the slice. Both estimators rely on restricted isotropy, which must be assured in applications. Note, however, that $\mathbf{K}_0$ need not be a body of revolution around the vertical axis, but only its distribution must be invariant under rotations, fixing this axis, see also Figure 4 below.

4 The Lévy particle model

We have compared by simulation the statistical behaviour of the section estimator and the slice estimator under a flexible Lévy particle model ([1], [7], [8]).

Under such a model, the random particle $\mathbf{K}_0$ is star-shaped with respect to a point $c_0 \in \mathbb{R}^3$ and distributed as $c_0+\mathbf{Z}$, where $\mathbf{Z}$ is modelled as a random deformation of a fixed particle Z_0, say, which is star-shaped relative to the origin o. The random set $\mathbf{Z}$ is also star-shaped with respect to o and therefore uniquely determined by its radial function $\mathbf{R} : \mathbb{S}^2 \to [0, \infty)$ relative to o. (Recall that $\mathbf{R}(u)$ is the distance from o to the boundary of $\mathbf{Z}$ in direction $u \in \mathbb{S}^2$.) In the model, the radial function $\mathbf{R}$ is given by

$$\mathbf{R}(u) = r(u)\mathbf{X}(u), \qquad u \in \mathbb{S}^2,$$

where $r : \mathbb{S}^2 \to [0, \infty)$ is the radial function of the fixed particle Z_0 and $\mathbf{X} : \mathbb{S}^2 \to [0, \infty)$ is an isotropic non-negative Lévy-based stochastic process on $\mathbb{S}^2$ of the form

$$\mathbf{X}(u) = \int_{\mathbb{S}^2} k(u, v)\mathbf{Y}(\mathrm{d}v).$$

Here, k is chosen as the von Mises-Fisher kernel ([6]) and $\mathbf{Y}$ is a Gamma Lévy basis. The parameters of the stochastic process $\mathbf{X}$ are chosen such that $\mathbb{E}V_3(\mathbf{K}_0) = V_3(Z_0)$. This ensures that $\mathbf{Z}$ is a random deformation of Z_0. For more details, see [13, Section 6].

The set-up is illustrated in Figure 3. We choose $x(\mathbf{K}_0) = o$ as the reference point for $\mathbf{K}_0$. If $c_0 \neq o$, the reference points of the particles in the resulting particle process may be non-centrally placed in the particles, as illustrated on the profile to the right in Figure 3. The restricted isotropy assumption is fulfilled if c_0 belongs to the vertical axis M and Z_0 is a solid of revolution around M.

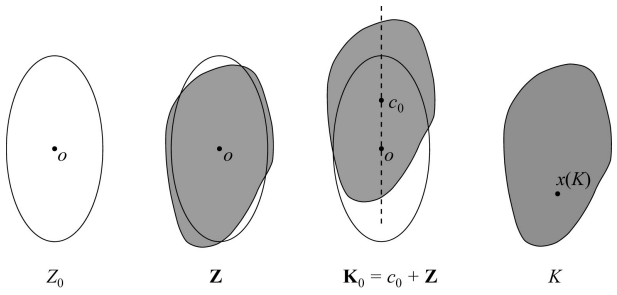

Figure 3: 2D illustration relating to the particle model, used in the simulation study. The typical particle $\mathbf{K}_0$ is distributed as $c_0 + \mathbf{Z}$ where $c_0 \in \mathbb{R}^3$ and $\mathbf{Z}$ is a random deformation of the ellipse Z_0. If $c_0 \neq o$, the reference points of the particles in the resulting particle process may be non-centrally placed in the particles, as illustrated on the profile to the right.

5 The simulation study

In this section, we compare by simulation the statistical behaviour of the slice estimator and the section estimator. We focus on the quality of the estimators of $\mathbb{E}\Phi_3^{r,0}(\mathbf{K}_0)$ for $r = 0, 1, 2$.

We use a Lévy particle model, fulfilling the restricted isotropy assumption. The fixed particle Z_0 is chosen as a prolate ellipsoid with its longest axis parallel to the vertical axis. The mean particle volume tensors $\mathbb{E}\Phi_3^{r,0}(\mathbf{K}_0)$, $r = 0, 1, 2$, determine the model parameters $v = \mathbb{E}\Phi_3^{0,0}(\mathbf{K}_0) = \mathbb{E}V_3(\mathbf{K}_0)$, $c_0 \in M$ and the lengths $a > b$ of the semi-axes of the ellipsoid Z_0. In the simulation study, we use the volume tensors to estimate this set of natural model parameters. Since $c_0 \in M$, $c_0 = ze$, where e spans M, so the focus is here on estimating z. In Figure 4, five replicated simulations of $\mathbf{K}_0$ are shown from the actual model used in the simulation study together with the ellipsoid Z_0 (left).

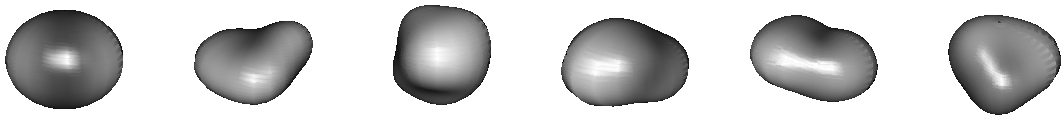

Figure 4: Particles simulated under the Lévy particle model as random deformations of a prolate ellipsoid. The ellipsoid is shown to the left, followed by five random deformations.

For a sample of n particles $\mathbf{K}_{01}, \ldots, \mathbf{K}_{0n}$, we have determined for $r = 0, 1, 2$

$$\frac{1}{n}\sum_{i=1}^{n} \widehat{\Phi}_3^{r,0}(\mathbf{K}_{0i}) \qquad \text{(the slice estimator)} \tag{5.1}$$

and

$$\frac{1}{n}\sum_{i=1}^{n} \widetilde{\Phi}_3^{r,0}(\mathbf{K}_{0i}) \qquad \text{(the section estimator)}. \tag{5.2}$$

In principle, the slice estimator (2.5) requires measurements in the whole slice T which typically covers the central half of the particle, as illustrated in Figure 5. In practice (and in the simulations), the slice is subsampled by a systematic set of parallel planes. We used three equidistant planes in T, as also shown in Figure 5. Each plane was subsampled by a systematic set of lines that was alternately parallel and perpendicular to the vertical axis. The distance between lines in a plane was chosen such that on the average two lines hit the particle in each plane. For more details, see [9, Fig. 2].

For the section estimator, $K_{0i} \cap L$ was subsampled by a systematic set of parallel lines in L, perpendicular to M. Again, the distance between lines was chosen such that on the average two lines hit the particle. With this set-up, the amount of work involved for the slice estimator is approximately three times that of the section estimator.

The simulation results for the slice estimator and the section estimator are shown in Tables 1 and 2, respectively, for the case of n=10, 20, 50 and 100 particles. For a

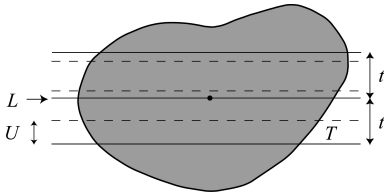

Figure 5: 2D illustration of the subsampling of a slice T of thickness $2t$. The slice is subsampled by three equidistant planes (shown as stippled lines) with distance $2t/3$ between neighbour planes. The position of the lower plane is determined by U which is uniform random in the interval $[0, 2t/3)$.

sample of n particles $\mathbf{K}_{01}, \ldots, \mathbf{K}_{0n}$, the estimators of v are

$$\widehat{v} = \frac{1}{n} \sum_{i=1}^{n} \widehat{\Phi}_3^{0,0}(\mathbf{K}_{0i}), \qquad \widetilde{v} = \frac{1}{n} \sum_{i=1}^{n} \widetilde{\Phi}_3^{0,0}(\mathbf{K}_{0i}), \tag{5.3}$$

depending on whether the slice estimator or the section estimator is used.

n	10	20	50	100
v	606.860 (0.151)	606.860 (0.095)	606.860 (0.067)	606.860 (0.047)
z	−0.073 (6.162)	−0.074 (4.021)	−0.074 (2.867)	−0.074 (2.034)
a	5.821 (0.082)	5.841 (0.054)	5.848 (0.039)	5.852 (0.028)
b	4.981 (0.068)	4.977 (0.044)	4.976 (0.031)	4.975 (0.022)

Table 1: For the slice estimator, we show the mean (and CV) of the estimated mean particle volume v, displacement z and semi-axis lengths $a > b$ of the prolate ellipsoid Z_0, determined from estimated mean volume tensors based on n simulated particles in $500\,000/n$ simulations. The true parameter values are $v = 606.553$, $z = -0.073$, $a = 5.857$ and $b = 4.972$. The parameter values resemble the ones obtained in concrete analyses of microscopy data. The ellipsoid Z_0 is shown to the left in Figure 4 followed by five random particles from the Lévy particle model, used in the simulation study. Estimation is done under the assumption of restricted isotropy.

n	10	20	50	100
v	606.333 (0.152)	606.333 (0.096)	606.333 (0.068)	606.333 (0.048)
z	−0.069 (7.057)	−0.069 (4.560)	−0.069 (3.258)	−0.069 (2.337)
a	5.797 (0.098)	5.832 (0.064)	5.844 (0.047)	5.850 (0.033)
b	4.992 (0.070)	4.981 (0.044)	4.976 (0.032)	4.974 (0.022)

Table 2: For the section estimator, we show the mean (and CV) of the estimated mean particle volume v, displacement z and semi-axis lengths $a > b$ of the prolate ellipsoid Z_0, determined from estimated mean volume tensors based on n simulated particles in $500\,000/n$ simulations. The true parameter values are given in the legend to Table 1.

Likewise, the estimators of z become

$$\widehat{z} = \frac{\frac{1}{n}\sum_{i=1}^{n} \widehat{\Phi}_3^{1,0}(\mathbf{K}_{0i})}{\frac{1}{n}\sum_{i=1}^{n} \widehat{\Phi}_3^{0,0}(\mathbf{K}_{0i})} \cdot e, \qquad \widetilde{z} = \frac{\frac{1}{n}\sum_{i=1}^{n} \widetilde{\Phi}_3^{1,0}(\mathbf{K}_{0i})}{\frac{1}{n}\sum_{i=1}^{n} \widetilde{\Phi}_3^{0,0}(\mathbf{K}_{0i})} \cdot e, \tag{5.4}$$

where e spans the vertical axis M. The estimators of the semi-axis lengths a and b of the ellipsoid Z_0 are non-linear functions of the estimators of mean particle tensors of rank 0,1 and 2.

A total of 500 000 particles was simulated. These particles are used in Table 1 and 2 to produce $500\,000/n$ samples of n particles. Since the same 500 000 particles are used for all n and the estimated mean particle volume is a simple average, according to (5.3), the mean of the estimated mean particle volume v in Table 1 and 2 does not depend on n. The mean of the estimated displacement z is also virtually constant which shows that for the model used in the simulation study the bias of the estimators of z in (5.4) is negligable, also for as small n as 10.

Table 1 and 2 show that both the slice estimator and the section estimator provide estimators of the mean particle volume v and the semi-axis lengths a and b of the prolate ellipsoid Z_0 with CVs less than 10 % if 20 or more particles are sampled while it is needed to sample more than 100 particles if the very small displacement z is to be discovered. Comparing the section estimator with n particles to the slice estimator with $n/3$ particles (same amount of work), the section estimator is superior.

6 Non-parametric inference

In the simulation study, we used the estimators of mean particle volume tensors $\mathbb{E}\Phi_3^{r,0}(\mathbf{K}_0)$, $r = 0, 1, 2$, to estimate the parameters in the simulated Lévy particle model. In cases where the particle model is not a suitable description of the particle population under consideration, we may still use the mean particle volume tensors to obtain information about particle size, position, shape and orientation. Here, $\mathbb{E}\Phi_3^{0,0}(\mathbf{K}_0) = \mathbb{E}V_3(\mathbf{K}_0)$ is, of course, a size parameter (mean particle volume) while $\bar{c} = \mathbb{E}\Phi_3^{1,0}(\mathbf{K}_0)/\mathbb{E}\Phi_3^{0,0}(\mathbf{K}_0)$ contains information about the deviation of the centre of gravity from the reference point of the typical particle. Likewise, we can use $\mathbb{E}\Phi_3^{r,0}(\mathbf{K}_0)$, $r = 0, 1, 2$, to construct an approximating ellipsoid $\bar{c}+\bar{e}$, say, that contains information about particle shape and orientation of the typical particle. Here, $\bar{e}$ is a centred ellipsoid, called the *Miles ellipsoid*. It can be constructed from a spectral decomposition of

$$\mathbb{E}\Phi_3^{2,0}(\mathbf{K}_0) - \frac{(\mathbb{E}\Phi_3^{1,0}(\mathbf{K}_0))^2}{2\mathbb{E}\Phi_3^{0,0}(\mathbf{K}_0)}.$$

For more details, see [13, Section 4.2 and 4.3].

Acknowledgements

We are grateful to Kaj Vedel for the skilful technical assistance with the graphical illustrations. This research was supported by Centre for Stochastic Geometry and Advanced Bioimaging, funded by the Villum Foundation.

References

[1] Barndorff-Nielsen, O.E., Schmiegel, J.: Lévy based tempo-spatial modeling; with applications to turbulence. Uspekhi Mat. Nauk. **159**, 63–90 (2004).

[2] Beisbart, C., Barbosa, M.S., Wagner, H., da F. Costa, L.: Extended morphometric analysis of neuronal cells with Minkowski valuations. Eur. Phys. J. B **52**, 531–546 (2006).

[3] Beisbart, C., Dahlke, R., Mecke, K.R., Wagner, H.: Vector- and tensor-valued descriptors for spatial patterns. In: Morphology of Condensed Matter. Lecture Notes in Physics **600**, pp. 249–271. Springer, Berlin (2002).

[4] Daley, D.J., Vere-Jones, D.: An Introduction to the Theory of Point Processes, Volume II: General Theory and Structure (2nd edition). Springer, New York (2008).

[5] Denis, E.B., Barat, C., Jeulin, D., Ducottet, C.: 3D complex shape characterizations by statistical analysis: application to aluminium alloys. Mater. Charact. **59**, 338–343 (2008).

[6] Hansen, L.V., Thorarinsdottir, T.L., Gneiting, T.: Lévy particles: modelling and simulating star-shaped random sets. CSGB Research Report **2011-04**.

[7] Hellmund, G., Prokesova, M., Jensen, E.B.V.: Lévy-based Cox point processes. Adv. Appl. Prob. **40**, 603–629 (2008).

[8] Jónsdóttir, K.Y., Schmiegel, J., Jensen, E.B.V.: Lévy-based growth models. Bernoulli **14**, 62–90 (2008).

[9] Rafati, A.H., Ziegel, J.F., Nyengaard, J.R., Jensen, E.B.V.: Stereological estimation of particle shape and orientation from volume tensors. J. Microsc., in press. DOI: 10.1111/jmi.12382 (2016).

[10] Schneider, R., Weil, W.: Stochastic and Integral Geometry. Springer, Heidelberg (2008).

[11] Schröder-Turk, G.E., Kapfer, S.C., Breidenbach, B., Beisbart, C., Mecke, K.: Tensorial Minkowski functionals and anisotropy measures for planar patterns. J. Microsc. **238**, 57–74 (2011a).

[12] Schröder-Turk, G.E., Mickel, W., Kapfer, S.C., Klatt, M.A., Schaller, F.M., Hoffmann, M.J.F., Kleppmann, N., Armstrong, P., Inayat, A., Hug, D., Reichelsdorfer, M., Peukert, W., Schwieger, W., Mecke, K.: Minkowski tensor analysis of cellular, granular and porous structures. Adv. Mater. **23**, 2535–2553 (2011b).

[13] Ziegel, J.F., Nyengaard, J.R., Jensen, E.B.V.: Estimating particle shape and orientation using volume tensors. Scand. J. Stat. **42**, 813–831 (2015).